Atmospheric Environment Vol. 17, No. 1, pp. 1–9, 1983
Printed in Great Britain.

0004–6981/83/010001–09 $03.00/0

COMPARISON OF OPACITIES MEASURED BY PORTABLE AND CROSS-STACK TRANSMISSOMETERS AT A COAL-FIRED POWER PLANT

TRACEY W. STEIG and MICHAEL J. PILAT
Department of Civil Engineering, University of Washington, Seattle, WA 98195, U.S.A.

(*First received* 29 *September* 1981; *in revised form* 15 *January* 1982 *and received for publication* 15 *March* 1982)

Abstract—Simultaneous measurements of the in-stack light transmittance with portable (short pathlength) and cross-stack transmissometers along with particle mass concentration and particle size distribution tests were conducted at a pulverized coal-fired boiler. The tests were performed on a large horizontal duct downstream of an electrostatic precipitator. The cross-stack transmissometer (one way pathlength of 6.15 m) was located horizontally across the center of the duct during the entire study. The portable transmissometer (one way pathlength of 1.27 m) was positioned horizontally at either the top, center or bottom sampling port. The one hour average opacities measured simultaneously with the portable and cross-stack transmissometers have correlation coefficients of the linear regression best fit lines in the 0.933–0.999 range compared to the one minute opacity correlation coefficients of 0.420–0.592. The higher correlation coefficients of the hourly averages are probably due to averaging the opacities over a time period longer than the precipitator rapping cycle of 12 min. The 1 min average cross-stack opacities were consistently greater than the portable opacities, probably caused by the cross-stack transmissometer seeing puffs of particles from the precipitator plate rapping. Vertical stratification of the particles was indicated by both the opacity and the particle mass concentration measurements.

NOMENCLATURE

b	light extinction coefficient of the aerosol (m^{-1})
f	fraction of total mass concentration
I	intensity of light transmitted through an aerosol
I_0	intensity of incident light upon the aerosol
K	ratio of the specific volume to the light extinction coefficient ($cm^3\,m^{-2}$)
L	light pathlength (m)
O	fractional opacity
R_b	$\overline{T_{cb}}/\overline{T_{pb}}$
R_c	$\overline{T_{cc}}/\overline{T_{pc}}$
R_t	$\overline{T_{ct}}/\overline{T_{pt}}$
T	fractional light transmittance
$\overline{T_c}$	average cross-stack transmittance during all tests (used as the reference transmittance) (fractional)
$\overline{T_{cb}}$	average cross-stack transmittance when the portable was at the bottom port (fractional)
$\overline{T_{cc}}$	average cross-stack transmittance when the portable was at the center port (fractional)
$\overline{T_{ct}}$	average cross-stack transmittance when the portable was at the top port (fractional)
$\overline{T_{pb}}$	average portable transmittance at the bottom port (fractional)
$\overline{T_{pc}}$	average portable transmittance at the center port (fractional)
$\overline{T_{pt}}$	average portable transmittance at the top port (fractional)
T_n	normalized light transmittance (fractional)
T_{nb}	normalized light transmittance at the bottom level (fractional)
T_{nt}	normalized light transmittance at the top level (fractional)
V_b	$\overline{W_b}/\overline{W_{cb}}$
V_t	$\overline{W_t}/\overline{W_{ct}}$
W	particle mass concentration (g/acm)
$\overline{W_b}$	average mass concentration at the bottom position (g/acm)
$\overline{W_{cb}}$	average mass concentration at the center position during mass concentration tests at the bottom position (g/acm)
$\overline{W_{ct}}$	average mass concentration at the center position during mass concentration tests at the top position (g/acm)
W_n	normalized particle mass concentration (g/acm)
W_{nt}	normalized mass concentration at the top level (g/acm)
W_r	average mass concentration at the center position for all tests (used as a reference mass concentration) (g/acm)
$\overline{W_t}$	average mass concentration at the top position (g/acm)
X	axis referring to the cross-stack transmittance (fractional)
Y	axis referring to the portable transmittance (fractional)
ρ	average particle density ($g\,cm^{-3}$).

1. INTRODUCTION

1.1. *Purpose of paper*

The purpose of this paper is to present the results of simultaneous measurements of instack opacity with a portable and a cross-stack light transmissometer on a horizontal duct downstream of an electrostatic precipitator at a coal-fired power plant. The use of continuous monitoring cross-stack light transmissometers to measure the instack opacity is of significance to providing information concerning both the plume opacity at the stack exit and the particle mass concentration to the power plant operator. Also, the EPA

New Source performance Standards (1971) require light transmissometers for instack opacity measurement on new coal and oil-fired steam generators.

The field study was conducted at a coal-fired power plant in order to determine whether portable light transmissometers would provide the same opacity readings as a cross-stack light transmissometer. A sampling location with vertical particle stratification (possibly due to particle settling), with horizontal stratification (caused by electrostatic precipitator plate rapping), uniform gas flow profile and a measurable opacity for the shorter portable transmissometer illumination pathlength was desired. Such a sampling location would thus indicate the possible magnitude of differences between the portable and cross-stack light transmissometers.

The results of this paper are of significance to the use of portable light transmissometers, to the location of transmissometers in ducts and stacks, and to the interpretation of opacity data.

1.2. *Review of literature*

1.2.1. *Transmissometers for opacity measurement.* Crider and Tash (1964) reported on the use of a light transmissometer to measure plume opacity. Conner and Hodkinson (1967) analyzed opacity, plume contrast, light transmissometers, telephotometers and discussed their relationship. Ensor and Pilat (1971) presented calculated effects of the light detector acceptance angle on the magnitude of the opacity measured by a light transmissometer. Peterson and Tomaides (1972) reported on experimental measurements of the effects of the light projection angle and the detector acceptance angle on the light transmittance for instack opacity measurements. Conner (1974) described two essential design criteria for light transmissometers for opacity measurement: (1) the spectral response should be in the visible range and (2) the transmissometer should have light collimating optics (i.e. have limited detector angle of view and limited light projection angle). Nader *et al.* (1974) discussed the proposed EPA transmissometer design and performance specifications prior to their promulgation in 1975. Avetta (1975) and Conner *et al.* (1979) analyzed these EPA transmissometer specifications and concluded that they were adequate for transmissometer opacity monitoring at the steel plant oxygen furnace and portland cement plants tested.

Gooch and Marchand (1978) reported on the performance testing of six utility coal-fired power plant electrostatic precipitators. A portable light transmissometer was used for measuring the opacity of the rapping puffs emitting from the precipitator. At one plant, 6 to 7 opacity puffs h^{-1} were measured. These puffs corresponded, approximately, to the rapping sequence of the collection plates on the outlet field of the electrostatic precipitator. Rapping puffs were measured with the portable transmissometer at the other five power plants tested. Problems in the opacity measurements were encountered with dust contamination of the transmissometer optics (which probably occurred during installation of the transmissometer probe into the duct while the plant is in operation).

1.2.2. *Federal law (EPA) requiring continuous opacity monitors on fossil fuel steam generators.* In 1971, the EPA promulgated "Standards of Performance for New Stationary Sources" which included requirements for the use of in-stack light transmissometers for monitoring opacity on fossil fuel steam generators. These "Standards of Performance for New Stationary Sources" have been revised several times since 1971 with the latest revision in 1980. The performance specifications for the in-stack light transmissometers were issued by EPA on 6 October 1975 (Title 40, Chapter 1, Appendix B). The transmissometer specifications include a calibration error of $\leqslant 3\%$ opacity, zero drift for a 24 h period of $\leqslant 2\%$ opacity, a response time maximum of 10 s, and an operational test period of 168 h to measure the performance of the instrument. The EPA also issued transmissometer design specifications in the same document. These include that the spectral response of the instrument have a mean and peak value between 500 and 600 nm with less than 10% of the spectral peak outside of the 400–700 nm wavelength range. The detector angle of view and the light projection angle cannot be greater than 5°.

1.2.3. *Gas flow stratification in ducts.* There are a number of reports on studies of the development of stack sampling procedures for situations of gas flow stratification. Zakak *et al.* (1974) examined SO_2 and CO_2 gas concentration gradients and velocity contours for stratified gas flow profiles in stacks. Crawford *et al.* (1975) and Brooks *et al.* (1975) showed by measuring SO_2 and NO (for stable CO_2 and O_2) that significant stratification of gas flows does occur in large power plants. Hanson *et al.* (1976) reviewed the literature concerning gas flow in ducts and profiles of gas flow and particle mass concentration gradients at large power plants (greater than 100 MW) and discussed stack sampling strategies. No data were found on the measurement of opacity in ducts with stratified gas velocity flow profiles.

1.2.4. *Opacity related to particle properties.* The transmission of light through an aerosol can be expressed in terms of the fractional light transmittance T by the Bouger law (Lambert–Beer Law)

$$T = \frac{I}{I_0} = \exp(-bL), \tag{1}$$

where b is the light extinction coefficient of the aerosol, L the illumination pathlength, I the intensity of the transmitted light, and I_0 the intensity of the incident light. The transmittance can be related to the opacity O by

$$O = 1 - T. \tag{2}$$

Pilat and Ensor (1970) have shown that the aerosol particle mass concentration W can be related to the light transmittance with a modification of the Bouger Law that takes into account the particle size distribution, particle refractive index, and light wavelength through the use of a parameter K,

$$\frac{I}{I_0} = \exp\left(-\frac{WL}{K\rho}\right) \tag{3}$$

where ρ is the average particle density and K is defined as the ratio of the specific particle volume to light extinction coefficient. Ensor and Pilat (1971) presented graphs for obtaining the magnitude of K as a function of the log normal particle size distribution parameters (mass mean radius and geometric standard deviation), the particle refractive index, and the light wavelength. For particle size distributions that are not log normal, Thielke and Pilat (1978) reported a method for calculating the opacity by dividing the particle size distribution into log normal segments and using a corresponding K for each segment.

The use of in-stack transmissometers for monitoring the particle mass concentration has been shown to be appropriate for some emission sources. Larssen *et al.* (1972) reported good correlation between particle mass concentration and in-stack light transmittance on the emissions from a pulp mill kraft recovery boiler. Other reports on in-stack opacity measurements correlated to particle mass concentration include Buhne and Duwell (1972) concerning a portland cement plant, Schneider (1974) about a coal-fired power plant, Cristello and Walther (1975) about two hog-fuel boilers and a kraft recovery boiler, Reisman *et al.* (1974) about a sludge incinerator and an oil-fired boiler, Conner *et al.* (1979) about oil-fired power plants and portland cement plants, and Conner and White (1981) about coal-fired power plants.

2. MEASUREMENT TECHNIQUES

2.1. *Test site*

The testing was conducted at the Centralia Steam-Electric Plant located near Centralia, Washington. The facility is a pulverized coal-fired electric power generating station owned by eight northwest utilities and operated by Pacific Power and Light Company. The plant has two identical boiler units which each have an electrical generating capacity of 665 MW. The coal has an average ash content of 13% (after washing) and a sulfur content of 0.5 to 0.8%.

The location of the testing was downstream of an one electrostatic precipitator and upstream of the second electrostatic precipitator on unit no. 1. As shown in Fig. 1, the gas flows from the boiler, through the first precipitator, upwards through a 90° turn, then some 18 m to the sampling location in the horizontal duct, then 9 m to a 45° upward bend in the duct, onwards through the second electrostatic precipitator, the ID fan, and up the stack. The horizontal duct where the testing was performed is 6.3 m wide by 4.9 m high (inside dimensions) with 0.3 m of insulation (6.9 by 5.5 m outside dimensions). The four sampling ports on the side of the duct at three levels were used for the transmissometer measurements. The ports on the top of the duct were used for particle mass concentration and size distribution tests. Figures 2 and 3 show the port locations and the particle sampling points in the duct.

2.2. *Sampling methods*

The particle mass concentration was measured with an EPA Method 17 sampling train (Lear Siegler PM-100 manual stack sampler and BGI TA-3 in-stack thimble filter holder). Binderless fiberglass thimbles 19 × 90 mm) were used in the filter holder. The sampling procedure used was in accordance with EPA Method 17 except that the samples were taken at one point rather than traversing the duct.

Two particle mass concentration sampling trains were operated simultaneously from the same top sampling port with one filter located in the vertical and horizontal center of the duct and the other filter positioned either 1.4 m above or below the center filter (depending on the plane of the portable transmissometer location). The locations of the sampling ports and the sampling points are shown in Figs 2 and 3.

The in-stack particle size distributions were measured with Mark 3 Pilat (University of Washington) Source Test Cascade Impactors (from Pollution Control Systems Corp.). Pilat *et al.* (1970) (1978) described the design and development of these cascade impactors. A Mark 3 Right Angle Entry attachment was used along with the cascade impactor and this attachment avoids having to use a buttonhook sampling nozzle. The attachment was used with a specially constructed short sampling nozzle of 0.635 cm diameter and 2.22 cm long, the short nozzle being necessary to fit through the 8.89 cm diameter sampling port. The particle size distribution tests were sampled at a constant gas flow rate which was ap-

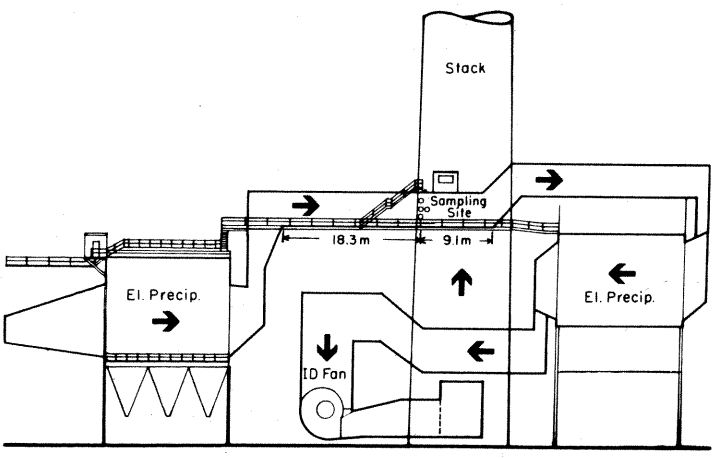

Fig. 1. Flow diagram of gas stream of Centralia Steam Plant.

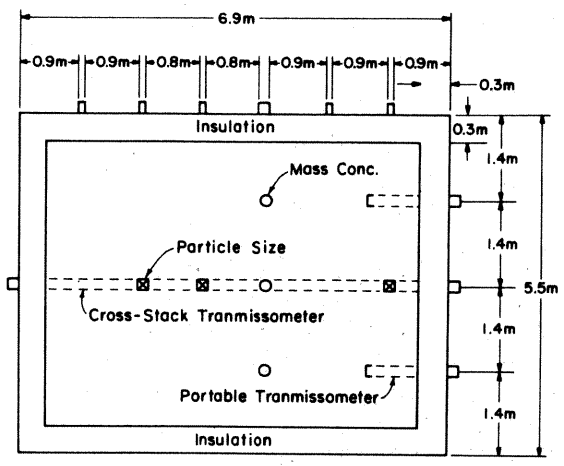

Fig. 2. Cross-section of duct showing sampling locations.

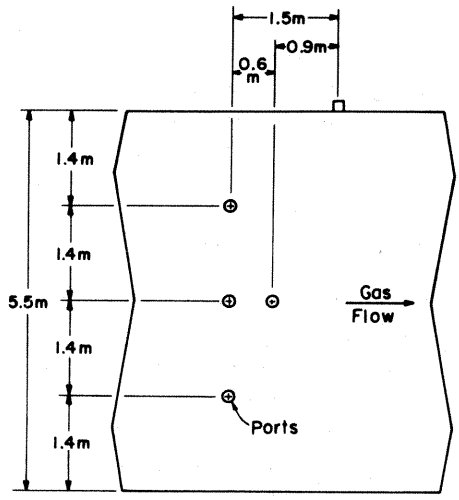

Fig. 3. Transmissometer sampling ports in side of duct.

proximately isokinetic. The Mark 3 Cascade impactor provided 8 particle size increments (7 jet stages plus the outlet filter) in the 0.2 to 15 μm aerodynamic cut diameter range.

The in-stack light transmittance was measured with a Lear Siegler RM-4 optical cross-stack transmissometer and a Lear Siegler RM-41 portable transmissometer. Beutner (1974) described the theory, design, and operation of the LSI RM-4 transmissometer. Both the RM-4 and RM-41P are double-pass electro-optical instruments which measure the attenuation of light through the gas stream and meet or exceed EPA performance specifications.

The RM-4 was mounted horizontally across the duct at the vertical center. The RM-41P was mounted horizontally in one of 3 side ports. The top port was 1.4 m above the center port. The RM-41P center port was along side the RM-4 instrument mounting position and the bottom port was 1.4 m below the center port. The effective in-stack pathlength for the RM-4 was 6.15 m (one way) and 1.27 m (one way) for the RM-41P. The opacity output was adjusted to 6.15 m pathlength for the portable transmissometer. The transmissometer mounting locations are shown in Figs 2 and 3.

3. RESULTS AND DISCUSSION

3.1. *Comparison of portable and cross-stack transmissometer opacities*

3.1.1. *One minute average opacities.* A comparison of the 1 min average opacities (adjusted pathlength of 6.15 m) measured by the portable and cross-stack transmissometers are shown for the three port locations in Figs 4–6. In each case the cross-stack

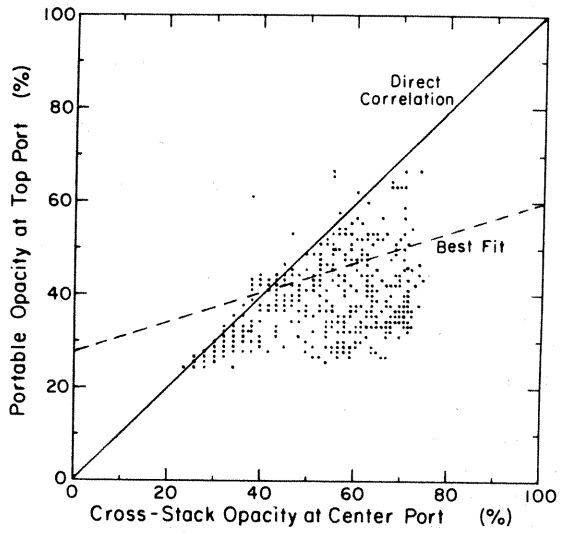

Fig. 4. One minute opacities of cross-stack (center port) and portable (top port) transmissometers.

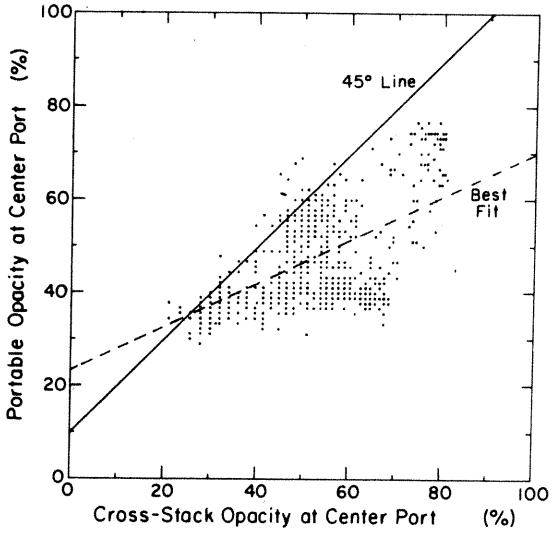

Fig. 5. One minute opacities of cross-stack (center port) and portable (center port) transmissometers.

transmissometer is in the center port. The best fit linear regression lines and correlation coefficients for the three port locations are presented in Table 1.

If there existed an uniform opacity across the duct,

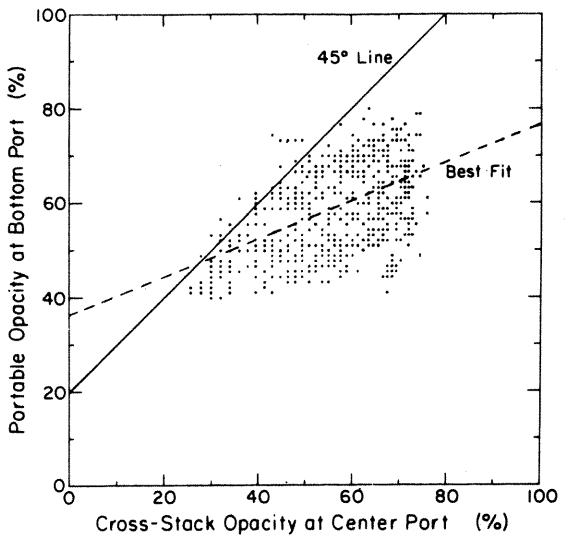

Fig. 6. One minute opacities of cross-stack (center port) and portable (bottom port) transmissometers.

Table 1. Best fit linear regression lines for one minute average opacities

Portable port location	Linear regression equation	Correlation coefficient
Top	*$Y = 0.28\,X + 23.58$	0.420
Middle	$Y = 0.47\,X + 22.75$	0.592
Bottom	$Y = 0.40\,X + 35.89$	0.538

* Y represents the portable and X represents the cross-stack opacity.

the portable and cross-stack opacity data would be expected to be located on the 45 degree direct correlation line of the graphs of Figs 4–6. With the portable in the top port, the opacity data in Fig. 4 shows the 45 degree direct correlation line is approximately an upper limit for the opacity comparison. Thus it appears that the cross-stack opacity is almost always greater than the portable opacity, at the top port.

With both the portable and cross-stack transmissometers at the center port, there is also an apparent 45 degree line upper boundary limit. However, this upper limit shows that at times the portable opacity exceeds the cross-stack opacity, as shown in Fig. 5. With the portable transmissometer in the bottom port, the upper 45 degree limit is moved further up with the magnitudes of the portable opacity increased.

The higher cross-stack opacity compared to portable opacity data points appear to be caused by horizontal stratification of the opacity. The electrostatic precipitator rapping cycle is such that the vertical plates are rapped in horizontal sections. Thus when a horizontal section on the side opposite from the location of the portable transmissometer is rapped, the opacity puff is measured by the cross-stack transmissometer but missed by the shorter probe of the portable transmissometer. The effective pathlength of the cross-stack transmissometer was about five times greater than the portable transmissometer (6.15 m across the duct one way compared to 1.27 m one way in the portable probe).

The few higher portable opacity compared to cross-stack opacity data points appear to be caused by rapping of the electrostatic precipitator on the same side as the portable transmissometer was located. The opacity puff is seen by both the portable and the cross-stack transmissometers, but the cross-stack had an illumination pathlength passing through the lower opacity non-puff region.

The electrostatic precipitator rapping cycle was about 12 min in duration, with the last row of collection plates each being rapped twice per cycle for 30 s every 4 and 8 mins.

3.1.2. *Hour average opacities.* A comparison of the one hour average opacities measured by the portable and cross-stack transmissometers for the three port locations are shown in Fig. 7. The data presented are 1 h average opacities of the 1 min transmissometer readings for each port location. In each case the cross-stack transmissometer was in the center port. The best fit linear regression lines and correlation coefficients for the three port locations are presented in Table 2.

The 1 h average opacity best fit lines in Fig. 7 show an increase in opacity from the top to the bottom of the duct and thus it appears that there was vertical opacity stratification in the duct.

The correlation coefficients between the opacities of the portable and the cross-stack transmissometers was higher for the 1 h averages (0.933 to 0.999) than for the 1 min averages (0.420 to 0.592). This is to be expected if

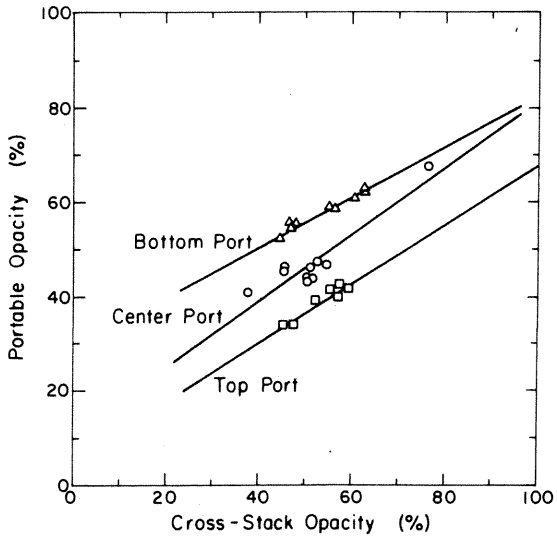

Fig. 7. One hour average opacities of cross-stack (center port) and portable (three ports) transmissometers.

Table 2. Best fit linear regression lines for hour average opacities

Portable port location	Linear regression equation	Correlation coefficient
Top	*$Y = 0.63\,X + 5.11$	0.971
Middle	$Y = 0.71\,X + 10.72$	0.933
Bottom	$Y = 0.53\,X + 28.94$	0.999

* Y represents the portable and X represents the cross-stack opacity.

the cause for the opacity fluctuations was the precipitator plate rapping. The plate rapping cycle for the entire precipitator is about 12 min. The strong correlation of the opacity hourly averages indicates the consistency of the rapping effect on the opacity.

3.2. *Particle mass concentration*

The particle mass concentration was measured from the same top port at three vertical positions. Three tests were taken at top and center locations and two tests were taken at the center and bottom locations, however all three locations were not measured simultaneously. There were large fluctuations in mass concentration results at the center of the duct for the six tests, however, there were mass stratification trends noted. For this reason, the data was normalized to show the trends. The average mass concentration at the center position for all the tests, W_r, was used as the reference mass concentration. The ratio of the average mass concentration at the top position, $\overline{W}_t$, compared to the average mass at the center position (during the same three tests), $\overline{W}_{ct}$, estimates the vertical mass stratification. The ratio, V_t, can be written as

$$V_t = \frac{\overline{W}_t}{\overline{W}_{ct}}. \tag{4}$$

This ratio was multiplied by the reference mass concentration to determine the normalized mass concentration at the top position, W_{nt}, and can be written as

$$W_{nt} = (V_t)(W_r). \tag{5}$$

The same procedure was used to determine a normalized mass concentration at the bottom position.

The results of the three simultaneous method 17 tests at the top and center position and two simultaneous tests at the center and bottom position of the duct, are shown in Table 3.

The normalized results show that the mass concentration increased from the top, to the center, to the bottom of the duct. Table 4 gives an indication of the vertical mass concentration stratification across the duct.

3.3. *Particle size distributions*

Three particle size distributions were measured by Pilat (University of Washington) Mark 3 cascade impactors simultaneously with opacity determinations made with the portable and cross-stack Lear Siegler transmissometers (which were located side by side in the vertical center of the duct). The impactor sampling points were all 2.5 m up from the bottom of the duct (at the vertical center) and at 3 horizontal locations (0.6, 3.2 and 4.0 m from the side of the duct where the portable transmissometer was located). These particle size distributions are shown in Fig. 8.

Table 5 presents the particle mass concentrations, cross-stack light transmittance, measured $K\rho$'s (calculated from particle mass concentration and cross-stack light transmittance at 6.147 m pathlength), and theoretical $K\rho$'s (calculated from particle size distributions and Mie light extinction equations). The measured $K\rho$'s were consistently lower in magnitude than the theoretical $K\rho$'s. This might be attributed to the particle density assumed in the theoretical calculation of $K\rho$ (particle density of $1.0\,g\,cm^{-3}$ was assumed in the computer calculations). The average light transmittance as measured by the cross-stack transmissometer was 0.502 and by the portable transmissometer was 0.560 over all three of the particle size tests.

3.4. *Light transmittance analysis*

The results of the comparison of the opacities measured by the portable and the cross-stack transmissometers show opacity stratification in both the vertical and horizontal directions. The magnitude of the vertical opacity stratification can be estimated by normalizing the portable and cross-stack opacities.

Table 3. Mass concentration as a function of position in duct

Particle mass concentration			Average mass concentration			Mass concentration ratio (fractional)
Top (g/acm)	Center (g/acm)	Bottom (g/acm)	Top (g/acm)	Center (g/acm)	Bottom (g/acm)	
0.170	0.272					
0.106	0.258		0.133	0.256		0.520 (V_t)
0.123	0.239		($\overline{W}_t$)	($\overline{W}_{ct}$)	($\overline{W}_b$)	
	0.098	0.127		0.068	0.145	2.127 (V_b)
	0.039	0.163		($\overline{W}_{cb}$)		

(W_r) 0.181 Average center mass concentration (reference).

Assuming that the opacity stratification horizontally across the duct is the same at the bottom, center and top port locations (i.e. vertically) and constant with time, the portable opacity readings at the three levels can be used to estimate the cross-stack opacity at these same levels.

The horizontal opacity stratification effect can be estimated by the ratio R_c of the average cross-stack transmittance $\overline{T}_{cc}$ to the average portable transmittance $\overline{T}_{pc}$ when both instruments were located adjacently at the center port.

$$R_c = \overline{T}_{cc}/\overline{T}_{pc}. \tag{6}$$

Because the cross-stack opacity was not constant as the portable opacity tests were conducted at the other two levels (top and bottom), a correction is needed for this variation. The ratio R_t of the average portable opacity at the top port $\overline{T}_{pt}$ compared to the average cross-stack transmittance at the center port (measured at the same time) $\overline{T}_{ct}$ is given as

$$R_t = \overline{T}_{pt}/\overline{T}_{ct}. \tag{7}$$

Using the average cross-stack transmittance $\overline{T}_c$ during all the tests as a reference, the normalized cross-stack transmittance at the top level T_{nt} is given by

$$T_{nt} = R_c R_t \overline{T}_c = \frac{\overline{T}_{cc}\overline{T}_{pt}}{\overline{T}_{pc}\overline{T}_{ct}}\overline{T}_c. \tag{8}$$

Thus, the cross-stack transmittance calculated from (8) is adjusted for both horizontal stratification across the duct and fluctuations between tests. This same normalization procedure was performed to obtain the cross-stack transmittance at the bottom level T_{nb}.

The average light transmittances and the portable to cross-stack transmittance ratios are presented in Table 6. The normalized transmittances and opacities are presented in Table 7.

Table 4. Normalized mass concentration as a function of position in duct

Vertical location	Normalized mass concentration (g/acm) (W_n)*
Top position	0.094
Center position	0.181
Bottom position	0.385

* 1 g/acm = 1 gram per actual cubic meter.

3.5. *Ratio of specific particle volume to light extinction coefficient*

Changes in the particle size distribution with vertical location in the duct can be estimated using the normalized particle mass concentrations W_n from

Table 5. Particle mass concentrations, light transmittance and $K\rho$'s

Test	Mass concentration (g/acm)	Light transmittance (fractional)	$K\rho$ measured ($g\,m^{-2}$)	$K\rho$ Theoretical ($g\,m^{-2}$)
J-1	0.074	0.513	0.683	1.136
J-2	0.100	0.506	0.905	1.470
J-3	0.098	0.487	0.835	1.261

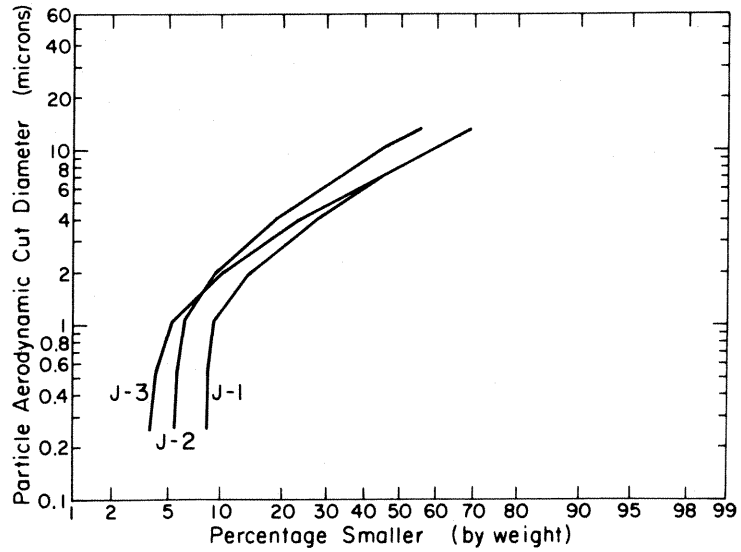

Fig. 8. Particle size distributions.

Table 6. Average light transmittance as a function of position in duct

Portable port location	Average light transmittance Portable (fractional)	Cross-stack (fractional)	Ratio of portable to cross-stack transmittance
Top	0.605 ($\overline{T}_{pt}$)	0.473 ($\overline{T}_{ct}$) (center)	1.279 (R_t)
Center	0.534 ($\overline{T}_{pc}$)	0.488 ($\overline{T}_{cc}$) (center)	0.914 (R_c)
Bottom	0.418 ($\overline{T}_{pb}$)	0.448 ($\overline{T}_{cb}$) (center)	0.933 (R_b)

Average cross-stack 0.470 ($\overline{T}_c$).

Table 7. Normalized light transmittance as a function of position in duct

Duct position	Normalized transmittance (fractional)
Top	0.549 (T_{nt})
Center	0.470 ($\overline{T}_c$)
Bottom	0.401 (T_{nb})

Table 4 and the normalized light transmittances T_n from Table 7 to calculate the ratio of the specific particle volume to light extinction coefficient times the particle density, $K\rho$. From Equation (3),

$$K\rho = -\frac{(W_n L)}{(\ln T_n)}$$

can be written, where W_n is the normalized mass concentration and T_n is the normalized light transmittance for a given position in the duct. Table 8 shows the combined term, $K\rho$, calculated for the three vertical duct locations.

The ratio of the specific volume to light extinction coefficient is a function of the particle size distribution as discussed by Pilat and Ensor (1970). The decrease in the measured $K\rho$ from the top to the bottom of the duct indicates that there was also a change in the particle size distribution at the three vertical locations. The measured geometric mass mean particle diameter ranged from 8.0 to 13.0 μm from the three cascade impactor tests (all taken at the center duct level). For particle size distributions with a geometric mass mean diameter of greater than about 1.0 μm, the ratio of the specific volume to light extinction coefficient increases as the geometric mass mean diameter increases.

Table 8. Ratio of specific particle volume to light extinction coefficient as a function of position in duct

Duct position	Normalized mass concentration (g/acm)	Normalized light transmittance (fractional)	$K\rho$ (g/m^{-2})
Top	0.094	0.549	0.965
Center	0.181	0.470	1.474
Bottom	0.385	0.401	2.591

Therefore it appears that the mass mean diameter of the particle size distribution increases from the top of the duct to the bottom.

3.6. *Performance of electrostatic precipitator*

The high mass concentration and opacity values indicate that the performance of the electrostatic precipitator had a large effect on the results. Gooch and Francis (1975) discussed velocity distribution, gas sneakage and particle re-entrainment as affecting the performance of precipitators. The dominant factor affecting the results of this study appear to be a result of particle re-entrainment caused by the collection plate rapping.

The collection plates were rapped at timed intervals across the electrostatic precipitator. The portable transmissometer would miss opacity puffs compared to the cross-stack when a collection plate would be rapped on the opposite side of the electrostatic precipitator. Therefore the horizontal stratification in this study appears to be a result of particle re-entrainment caused by the precipitator collection plate rapping cycle.

During a plant shutdown, a large layer of flyash (15–20 cm) was found to have built up on the bottom of the duct. Therefore, there were particles in the gas stream large enough to settle out during operation. A scouring action by the gas stream would tend to re-entrain the particles on the bottom of the duct. These two actions (settling and re-entrainment) would both contribute to the vertical particle stratification.

4. CONCLUSIONS

Based on the simultaneous measurements of the in-stack light transmittance with both the portable and cross-stack transmissometers, of the particle mass concentrations, and of the particle size distributions the following conclusions were made.

(1) The 1 h average opacities measured simultaneously by the portable (located at the three port levels) and the cross-stack transmissometer (located at the center level) have correlation coefficients in the 0.933–0.999 range. The high correlation coefficients for the 1 h average opacities were due to the 1 h averaging times being greater than the precipitator plate rapping cycles.

(2) The 1 min average opacities measured simultaneously by the portable and cross-stack transmissometers have correlation coefficients in the 0.420–0.592 range. The low correlation coefficients for the 1 min averages appear to be the result of the plate rapping cycle time being greater than the 1 min averaging time.

(3) Both the 1 min average opacities and the 1 h average opacities measured by the portable transmissometer were greater in magnitude at the bottom port level compared to the top port level, probably caused by vertical stratification of the particles (particles settling out).

(4) The 1 min cross-stack opacity was consistently greater than the portable opacity, possibly as the result of the cross-stack seeing puffs of particles caused by precipitator plate rapping.

(5) Normalized particle mass concentrations of 0.09 to 0.39 g/acm from the top level to the bottom level showed that vertical stratification of the particle mass concentration probably occurred.

(6) The magnitude of measured $K\rho$'s from the cross-stack transmittance and particle mass concentration measured simultaneously at the center level ranged from 0.68 to 0.90 $g\,m^{-2}$ and were consistently lower in magnitude than the theoretically calculated values.

(7) The magnitude of the measured $K\rho$'s from the portable transmissometer opacities (at top, center and bottom levels) and particle mass concentrations (center level) normalized to take into account the stratifications and fluctuations ranged from 0.96 to 2.59 $g\,m^{-2}$ from the top to bottom level, which indicates an increase in the particle size from top to bottom

Acknowledgements—The authors appreciate the assistance, advice and cooperation of our EPA Project Officer, William D. Conner. The cooperation of Ted Phillips and Tom White of the Pacific Power and Light Co. was very helpful. The valuable assistance of Lear Siegler, Inc. in providing a longer probe for the portable transmissometer, along with helpful advice, was greatly appreciated. The assistance of University of Washington students including Gary Raemhild, Peter Mincey and Jim Wilder is acknowledged. This research was supported under EPA Grant No. R803897.

REFERENCES

Avetta E. D. (1975) "In-stack transmissometer evaluation, and application to particulate opacity measurement. EPA Report No. EPA-650/2-75-008. NTIS PB 242-934.

Beutner H. P. (1974) Measurement of opacity and particulate emissions with an in-stack transmissometer. *J. Air Pollut. Control Ass.* **24,** 865–871.

Brooks E. F., Flegal C., Harnett L., Kolpin M., Luciani D. and Williams R. (1975) Continuous measurement of gas composition from stationary sources. EPA Report No. EPA-600/2-75-012.

Buhne K. W. and Duwell L. (1972) Recording dust emission measurements in the cement industry with the RM-4 smoke density meter made by Messrs Sick. *Staub* **32,** 19–26.

Conner W. D. (1974) Measurement of the opacity and mass concentration of particulate emissions by transmissometry. EPA Report No. EPA-650/2-74-128.

Conner W. D. and Hodkinson J. R. (1967) Optical properties and visual effects of smoke plumes. USPHS Pub. No. 999-AP-30.

Conner W. D., Knapp K. T. and Nader J. S. (1979) Applicability of transmissometers to opacity measurements of emissions—oil fired power boilers and portland cement plants. EPA Report No. EPA-600/2-79-188.

Conner W. D. and White N. (1981) Correlation between light attenuation and particulate concentration of a coal-fired power plant emission. *Atmospheric Environment* **15,** 939–944.

Crawford A. R., Gregory M., Manny E. and Bartok W. (1975) Magnitude of SO_2, NO, CO_2 and O_2 stratification in power plant ducts. EPA Report No. EPA-600/2-75-053.

Crider W. L. and Tash J. A. (1964) Study of vision obscuration by nonblack plumes. *J. Air Pollut. Control Ass.* **14,** 161–165.

Cristello J. D. and Walther J. E. (1975) Continuous on stack monitoring of particulate proves feasible. *Pulp Paper* **49,** 122–124.

Ensor D. S. and Pilat M. J. (1971) Calculation of smoke plume opacity from particulate air pollutant properties. *J. Air Pollut. Control Ass.* **21,** 496–501.

Gooch J. P. and Francis N. L. (1975) A theoretically based mathematical model for calculation of electrostatic precipitator performance. *J. Air Pollut. Control Ass.* **25,** 108–118.

Gooch J. P. and Marchant G. H. (1978) Electrostatic precipitator rapping re-entrainment and computer model studies. EPRI Report No. FP-792, Vol. 3.

Hansen H. A., Davine F., Morgan J. and Iversen A. (1976) Particulate sampling strategies for large power plants including non-uniform flow. EPA Report No. EPA-600/2-76-170.

Larssen S., Ensor D. and Pilat M. (1972) Relationship of plume opacity to the properties of particulates emitted from kraft recovery furnaces. *TAPPI* **55,** 88–92.

Nader J., Jaye F. and Conner W. (1974) Performance specifications for stationary source monitoring systems for gases and visible emissions. EPA Report No. EPA-654/2-74-013. NTIS PB 230–934.

Pilat M. and Ensor D. (1970) Plume opacity and particle mass concentration. *Atmospheric Environment* **4,** 163–173.

Pilat M., Ensor D. and Bosch J. (1970) Source test cascade impactor. *Atmospheric Environment* **4,** 671–679.

Pilat J., Raemhild G., Powell E., Fioretti G. and Meyer D. (1978) Development of a cascade impactor system for sampling 0.02 to 20.0 micron diameter particles. EPRI Report No. FP-844, Vol. 1.

Reisman E., Gerber W. and Potter N. (1974) In-stack transmissometer measurement of particulate opacity and mass concentration. EPA Report No. EPA-650/2-74-120. NTIS PB 239–864.

Schneider W. A. (1974) Opacity monitoring of stack emissions: a design tool with promising results. *The* 1974 *Electric Utility-Generation Planbook*, pp. 73–75. McGraw-Hill, New York.

Thielke J. and Pilat M. (1978) Plume opacity related to particle mass concentration and size distribution. *Atmospheric Environment* **12,** 2439–2447.

U.S.EPA (1971) Standards of performance for fossil fuel steam generators. *Fedl Register* Title 40, Part 60, Subpart D. (Dec. 23, 1971).

U.S.EPA (1975) Standards of performance for fossil fuel steam generators. *Fedl Register* Vol 40, No. 194, 46259–46263 (Oct. 6, 1975).

Zakak A., Siegel R., McCoy J., Arab-Ismali S., Porter J., Harris L., Forney L. and Lisk R. (1974) Procedures for measurements in stratified gases. VEPA Report No. EPA-650/2-74-086a, b.